Hypersonic minimum drag forebodies with blunt leading edges

J. Pike
jack@jackpike.co.uk
Bedfordshire, UK

ABSTRACT

The minimum pressure drag of blunt forebodies in hypersonic flow is investigated using Newton's Impact Theory. It is shown how the minimum drag shape varies with the body slenderness and the amount of blunting. As the blunting increases the drag approaches that of the minimum drag axisymmetric body.

NOMENCLATURE

C_D	drag coefficient of blunt spatula forebody with base area as reference area
C_{Daxi}	drag coefficient of minimum drag axisymmetric forebody with base as reference area
k	constant of Newton Impact theory (usually two or the stagnation pressure)
r	radius of axisymmetric body
r_O	radius of axisymmetric body at $x = 0$
x	streamwise co-ordinate from the forebody nose
θ	angle of inclination of body surface to the flow direction
τ	forebody base diameter over length

Subscript

b	base value

Paper No. 3828. Manuscript received 13 March 2011, revised version received 19 June 2012, accepted 18 October 2012.

1.0 INTRODUCTION

At hypersonic speeds, minimum drag forebodies of given length have a flat spatula shape with sharp leading edges[1]. However the effect of aerodynamic heating at hypersonic speeds may require the leading edges to be blunt[2,3]. This requirement could increase the drag sufficiently for the optimum shape to revert from the spatulate shape to an axisymmetric minimum drag shape similar to those found by Newton[4]. The effect of blunting on the minimum pressure drag spatulate shape is considered here for forebodies of various slenderness using Newton's Impact theory. The drag is compared with that of Newton's[4] minimum drag axisymmetric body shapes, where the shapes[5] and pressure drag coefficients[6] are available as analytical expressions depending on the slenderness ratio. Correlating these expressions[5,6], we have for a surface pressure coefficient given by $k\mathrm{Sin}^2\theta$, that the body geometry, drag coefficient and slenderness ratio for the axisymmetric bodies are given in terms of the surface slope and slope at the base by

$$\frac{r}{r_o} = \frac{1}{4}\mathrm{Sec}\theta\mathrm{Cosec}^3\theta \qquad \ldots (1)$$

$$\frac{x}{r_o} = \frac{1}{16}(3\mathrm{Cot}^4\theta + 4\mathrm{Cot}^2\theta - 7 + \mathrm{Ln}(\mathrm{Tan}\theta)) \qquad \ldots (2)$$

$$C_{Daxi} = k\mathrm{Sin}^2\theta_b(1-(4/\tau)\mathrm{Sin}\,\theta_b\,\mathrm{Cos}\,\theta_b + 2\mathrm{Cos}^2\theta_b) \qquad \ldots (3)$$

$$\tau = \frac{2r_b}{x_b} = \frac{8\mathrm{Tan}\theta_b}{3-2\mathrm{Sin}^2\theta_b - 4\mathrm{Sin}^4\theta_b(2-\mathrm{Ln}(\mathrm{Sin}\theta_b))} \qquad \ldots (4)$$

Although Newton derived his bodies without the bluntness constraint, a small flat region naturally occurs at the nose, such that applying a bluntness constraint to these bodies for the amounts of bluntness considered here makes little or no difference to the drag coefficient of these bodies.

The minimum drag of the more general blunt bodies is found by making local changes in the shape and retaining them if they reduce in the drag. This technique depends upon the local nature of Newtonian theory and has been successfully used previously for sharp leading edge

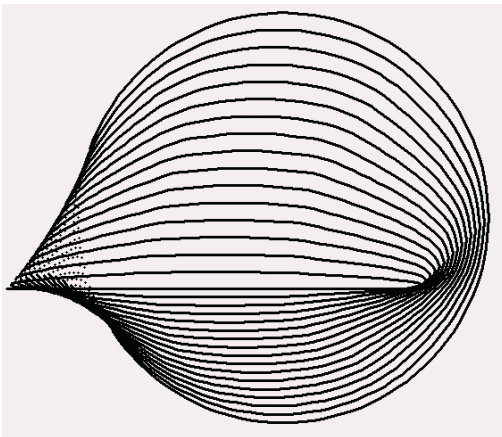

Figure 1. Sharp leading edge body with τ = ½.

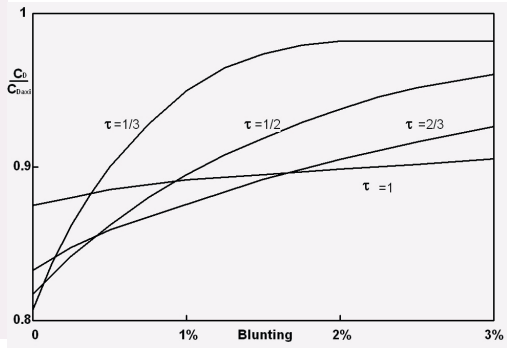

Figure 2. Drag coefficient compared with an axisymmetric minimum drag forebody.

https://doi.org/10.1017/S0001924000008186 Published online by Cambridge University Press

bodies[1]. A three-quarter front view of a typical inviscid sharp leading edge minimum drag spatula shape derived by this technique[1] is shown in Fig. 1. The curves show the shape of the body at 16 equally spaced cross-sections as the body expands from the sharp leading edge to the circular base.

In Fig. 2 the drag coefficients are compared with that of the minimum drag axisymmetric bodies with the same slenderness ratio. The comparative drag coefficient of the body of Fig. 1 and similar sharp leading edge bodies of different slenderness, are shown in Fig. 2 by the intersection of the curves with the left hand vertical axis. The results for forebodies with τ values of 1, ⅔, ½ and ⅓ are shown, representing bodies which have lengths of 2, 3, 4 and 6 times the base radius and axisymmetric drag coefficients of 0·321, 0·165, 0·0981 and 0·0454 respectively. For sharp leading edge bodies, we see from the vertical axis in Fig. 2, that as the forebodies become more slender their drag coefficient decreases from about 88% of that of the equivalent axisymmetric body when $\tau = 1$ to nearly 80% when $\tau = ⅓$.

Newtonian impact theory has a constant (k) associated with the surface pressure coefficient on the body which has a direct effect on the drag coefficient. Traditionally k has the value of 2, representing the limit of the stagnation pressure coefficient for infinite Mach number and a ratio of specific heats of unity. A more realistic value for k when considering blunt configurations is to put k equal to the flow stagnation pressure coefficient. Although the particular value of k used effects the value of the drag coefficient it does not affect the shape of the minimum drag shape. The drag dependency on the value of k is removed by comparing the drag coefficient with that of a reference shape as in Fig. 2, so that the optimisation becomes independent of the value of k. It should be noted also, that because all the drag coefficients use the base area as reference, the drag ratio is the same as the drag coefficient ratio.

2.0 BLUNT LEADING EDGE BODIES

When the leading edge of the shape shown in Fig. 1 is blunted without otherwise optimising its shape, the drag rapidly increases such that any advantage over the axisymmetric shape is soon lost.

However blunting in this manner does not give the minimum drag. To find the minimum drag, the blunting needs to be included within the optimisation process, which is achieved here by applying a maximum surface curvature constraint on the body surface throughout the optimisation. The resulting minimum drag coefficients are shown in Fig. 2 for a range of forebodies. The horizontal axis gives the blunting radius of curvature as a percentage of the base radius and the vertical axis shows the pressure drag coefficient compared with that of the

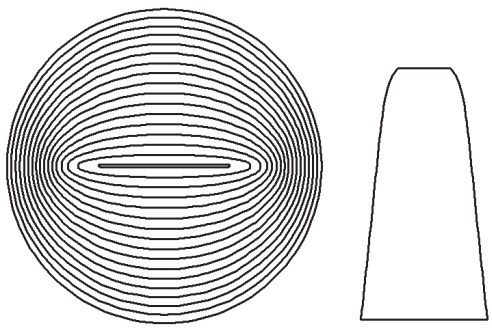

Figure 3. Minimum drag forebody with $\tau = ½$ and 1% blunting.

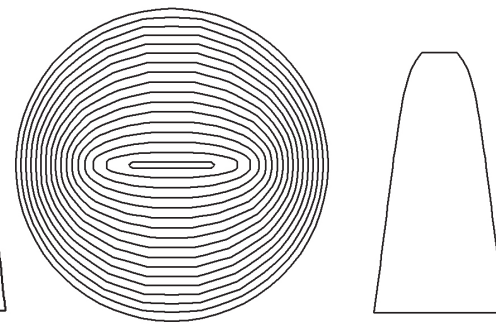

Figure 4. Minimum drag forebody with $\tau = ½$ and 2% blunting.

https://doi.org/10.1017/S0001924000008186 Published online by Cambridge University Press

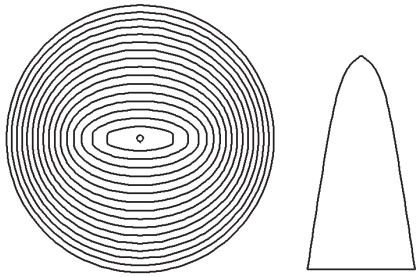

Figure 5. Minimum drag forebody with τ = ½ and 3% blunting.

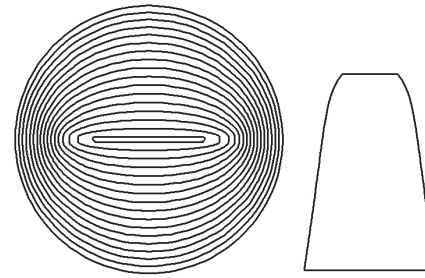

Figure 6. Minimum drag forebody with τ = ⅔ and 2% blunting.

minimum drag axisymmetric body. We see that the drag coefficient increases with the blunting radius for all the bodies, but the variation of the drag coefficient with the blunting depends on the slenderness of the body. For the most slender bodies (τ = ⅓), the drag advantage over the axisymmetric body is rapidly eroded. For less slender bodies the effect is less, with the blunting having less impact on the drag when τ = 1.

The changes in the shape vary as the blunting is increased from the sharp spatula body shown in Fig. 1 through to 'flattened' versions of the axisymmetric bodies. This shape change is shown in Figs 3 to 5 for τ = ½ with blunting of 1%, 2% and 3% of the base radius. Even a 1% blunting causes a reduction in the width of the spatula nose, from the full width shown in Fig. 1 to that of Fig. 3. By 2% blunting the flattened body shape is retained, but more of the body is swept as shown in Fig. 4. However, the pressure drag is still some 9% less than that of the axisymmetric body. Finally by 3% blunting, the body, as shown in Fig. 5, has become a flattened shape with a hemispherical nose.

Alternatively varying the body slenderness with a constant blunting at 2%, we see from Figs 6, 4 and 7 that the planform shape becomes more swept for the more slender bodies and from Fig. 2 the drag coefficient becomes closer to the axisymmetric value.

Consideration is given here to spatula shapes which minimise the forebody pressure drag upstream of a circular base, however in general other requirements on the forebody will modify the shape[7,8]. As can be seen in Figs 3 to 7, spatula bodies tend to have greater wetted area, plan area and volume than the axisymmetric body with the same slenderness and blunting. The increase in the volume or plan area could be an advantage for some applications, but the increase in the wetted area could disadvantage spatula bodies by increasing the friction drag. For example, the body with τ = ½ and 2% blunting shown in Fig. 4 has a wetted area 8% greater than the axisymmetric body. In this case should the friction drag is greater than the pressure drag, the

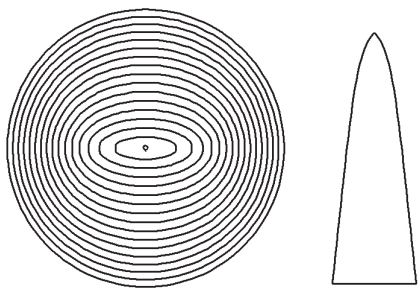

Figure 7. Minimum drag forebody with τ = ⅓ and 2% blunting.

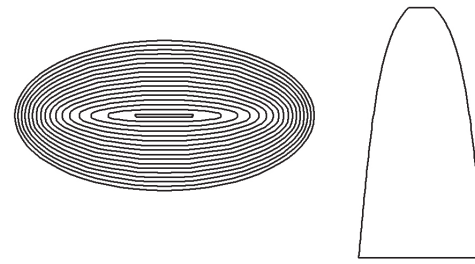

Figure 8. Blunt spatula body with an elliptical base.

https://doi.org/10.1017/S0001924000008186 Published online by Cambridge University Press

axisymmetric body may well have the lesser total drag, although this precludes any optimisation of spatula body shape to reduce the total drag.

For non-circular bases the minimum drag shapes are modified, but they still tend to have similar spatula noses. Figure 8 shows the minimum drag shape with an ellipse base where the minor axis is half the major axis. The τ value is ½ based on the major axis and the blunting radius is 2% of the minor axis or 1% of the major axis. We see that the extent of the unswept leading edge is similar to that of Fig. 4 but the planform is less swept near the nose. The pressure drag coefficient is 0·037, which is 24% less than the minimum drag axisymmetric body with the same length and base area or 26% less than the equivalent self-similar minimum drag elliptical body.

Further investigation of the effect of including friction drag and the effect of other base shapes would be useful. Also the accuracy of the drag coefficient of spatula shapes could be improved by using a more accurate flow calculation method. However to modify the shapes to further reduce the drag using a more complex method would be difficult, but a hybrid method which perturbs a known accurate solution may be possible.

3.0 CONCLUSIONS

Blunt minimum pressure drag forebodies at hypersonic speeds can have a spatula planform with a blunt leading edge normal to the flow. Results are presented for circular base bodies for a range of body lengths and bluntness.

The extent of the blunt unswept leading edge decreases with increasing bluntness until the shape reverts to a spherical nosed body. The change in the shape occurs more rapidly for more slender bodies. For a blunting of 3% of the base radius, a body of length 4 times the base radius becomes a flattened spherically nosed body.

The drag can be up to 20% less than the axisymmetric minimum drag shape but the difference reduces with increasing blunting. A spatula body of length four times the base radius and 2% blunting has a pressure drag 9% less than the equivalent minimum drag axisymmetric body.

Although the spatula shape variation is shown for circular based bodies, it is indicated how elliptical base shapes with a minimum drag coefficient have similar spatula noses.

REFERENCES

1. PIKE, J. Minimum drag bodies of given length and base using Newtonian theory, *AIAA J*, June 1977, **15**, (6), pp 769-770.
2. ANDERSON, J.D. Jr *Hypersonic and High Temperature Gas Dynamics,* McGraw-Hill Series in Aeronautical and Aerospace Engineering, New York, USA, 1989.
3. QUINN, R.D. and GONG, L. Real-Time Aerodynamic Heating and Surface Temperature Calculations for Hypersonic Flight Simulation, NASA TM 4222, August 1990.
4. NEWTON I. *Mathematical Principles of Natural Philosophy*, A. Motte's translation revised by CAJORI, F., University of California Press, Berkeley, California, USA, 1934.
5. PIKE, J. Minimum forebody drag in hypersonic continuum and rarefied flows, *Aeronaut J*, June 2006, **110**, (1108), pp 369-374.
6. EGGERS A.J., RESNIKOFF M.M. and DENNIS D.H. Bodies of revolution having minimum drag at high supersonic airspeeds, NACA TN 3666, February 1956.
7. TOWNEND, L.H. Hypersonic aircraft: lifting re-entry and launch, Philosophical Transactions of the Royal Society, Series A, August 1999, **357**, (1759), pp 2135-2389.
8. CZYSZ, P.A. and BRUNO, C. *Future Spacecraft Propulsion Systems*, Springer, New York, USA, Praxis, Chichester, UK, 2009.

https://doi.org/10.1017/S0001924000008186 Published online by Cambridge University Press